ELSEVIER

Tectonophysics 305 (1999) 371–379

TECTONOPHYSICS

Fault geometry and earthquakes in continental interiors

Pradeep Talwani *

Department of Geological Sciences, University of South Carolina, Columbia, SC 29208, USA

Received 1 May 1998; revised version received 30 June 1998; accepted 1 August 1998

Abstract

Although large earthquakes in continental interiors are much less frequent than those along plate boundaries, they have been responsible for a disproportionate amount of destruction. I present a testable model for strain accumulation and seismicity in the upper crust of continental interiors. Intersecting faults provide a focus for strain build-up, resulting in local pockets of high strain accumulation. Rigid plates typically deform at strain rates 10^{-10} to 10^{-9} strain yr^{-1}, but at intersecting fault zones, strain accumulates at anomalously high rates of 10^{-8} to 10^{-7} strain yr^{-1}, i.e., the strain rates are comparable with those at plate boundaries. The resulting large earthquakes are associated with relatively short return times (hundreds of years). Typically one of the intersecting faults appears to split and to offset the other 'main' fault (defined as a fault on which the larger offset occurs), forming two parallel strands separated by a jog. I also observe a rotation of one leg of the 'main' fault with respect to the other. The region of intersection is usually associated with intense fracturing, increased microseismicity and uplift.

Keywords: intraplate earthquakes; fault geometry; New Madrid earthquake; Charleston; South Carolina earthquake

1. Introduction

Although only about 5% of the global seismic energy is released in continental interiors, some of the most damaging earthquakes have occurred there. The nature of the seismicity in continental interiors is not as well understood as that of its plate boundary counterparts.

Several factors influence earthquake generation including the rheological properties of the medium, the nature of the fault zone, stress conditions, etc. However, my main focus is the effect of fault geometry (in a given stress field) on the generation and localizing of earthquakes, in particular, on the role of intersecting faults.

Fault intersections control earthquake occurrence in many ways. They provide locations for initiation and cessation of ruptures (King, 1986), thus controlling the size of the earthquakes. Intersections also control earthquake sequences by loading or unloading stresses on adjacent (or intersecting) faults (see e.g., King et al., 1994). Intersections also provide localized weak spots compared to the more compact regions and are thus likely to be the location of seismicity. Fault intersections are also regions of greater fracture density (Talwani, 1989; Marshak and Paulsen, 1997) thus promoting fluid flow, increased fluid pressure, lower strength and subsequent seismicity. However, the main thrust of this paper is the role of fault intersections in concentrating stress and generating earthquakes.

The roles of intersecting faults are observed in a variety of tectonic settings; at plate boundaries

* Tel.: +1 803 777 6449; Fax: +1 803 777 6610; E-mail: talwani@prithvi.seis.sc.edu

0040-1951/99/$ – see front matter
PII: S0040-1951(99)00024-4

(e.g., 1987 Superstition Hills earthquake sequence; Hudnut et al., 1989), in rift structures (e.g., Sudan earthquake sequence of 1990–91; Girdler and McConnell, 1994) and in continental interiors.

In this paper I present a simple, speculative, testable model primarily to explain the seismicity in the New Madrid and Middleton Place Summerville (near Charleston, South Carolina) seismic zones. It is based on the intersection model (Talwani, 1988) and theoretical modeling of stress fields near fault bends and intersections (King, 1986; Andrews, 1989, 1994; Jing and Stephansson, 1990). The model is constrained by observations of the seismicity patterns, regional and continental geodetic strain rates and recent estimates of recurrence times of large earthquakes based on paleoseismic studies.

1.1. Intraplate strain rates

On a global scale, seismicity in continental interiors is clustered, although locally, it can display linear patterns, e.g., the seismicity in the New Madrid Seismic Zone (NMSZ). Most of this seismicity occurs in the upper crust. Johnston (1994) compiled data for seismicity in stable continental regions (SCR), a more restrictive delineation of continental interiors. He found that the annualized seismic strain rates for all SCR regions was $\sim 1.3 \times 10^{-10}$ strain yr^{-1}. Direct measurements of baselines across the U.S. interior were made by Very Long Baseline Interferometry (VLBI). The data show the baseline lengths changing by less than 3 mm/yr, corresponding to a net strain less than 10^{-9} strain yr^{-1} (see e.g., Stein, 1993). Combined VLBI and satellite laser ranging (SLR) data for the central and eastern part of the United States also show deformation rates of less than 3 mm/yr (Robbins et al., 1993). Anderson (1986) estimated the average seismic strain rate for the central and eastern U.S. of 10^{-12} to 10^{-11} strain yr^{-1} from cumulative earthquake seismic moments, with large uncertainties of one to two orders of magnitude. These values are significantly smaller than the strain rates at plate boundaries $\sim 10^{-7}$ strain yr^{-1} (Johnston, 1994). The low strain rates suggest that on a continental scale, plate interiors (in this case, the North American plate) behaves as a single rigid plate. These conclusions based on the analysis of VLBI and SLR data have been confirmed by recent Global Positioning System (GPS) data (see e.g., Dixon et al., 1996; Snay and Strange, 1997).

1.2. Pockets of high strain rates within continental interiors

Although strain is a dimensionless quantity, I follow Savage (1983) and Weber et al. (1998) and use units of rad and rad per year for engineering shear strain (γ) and shear strain rate ($\dot{\gamma}$). These are distinguished from linear strain (ϵ) and linear strain rate ($\dot{\epsilon}$) expressed in units of strain and strain per year. Extension is taken as positive. These strains are related, the engineering shear strain is twice the corresponding tensor shear strain (Savage, 1983). Weber et al. (1998) have shown that the maximum shear strain rate ($\dot{\gamma}$, in rad yr^{-1}, $\dot{\gamma} \leq 2\dot{\epsilon}_{\max}$ where $\dot{\epsilon}_{\max}$ is the maximum principal strain rate (strain yr^{-1}).

Although the average strain rate in eastern U.S. from seismicity data is 10^{-12} to 10^{-11} strain yr^{-1}, Anderson (1986) also identified pockets of high seismic strain rates $\sim 10^{-8}$ strain yr^{-1} and 10^{-9} strain yr^{-1} in the New Madrid Seismic Zone (NMSZ) and Middleton Place Summerville Seismic Zone (MPSSZ) near Charleston, South Carolina, respectively. These high values were directly attributable to a series of large earthquakes ($M_w \sim 8$) in NMSZ in 1811–1812 and the M_w 7.3 1886 earthquake in the MPSSZ.

Strain rates based on geodetic data have also been obtained for small regions within continental interiors. In New York and Connecticut, Zoback et al. (1985) obtained a shear strain rate of 0.18 ± 0.05 μrad yr^{-1} ($\sim 10^{-7}$ strain yr^{-1}) by measuring changes in angles between monuments in two triangulation surveys (1862–1973). However, using a larger data set, Snay (1986) obtained a shear strain rate of 0.032 ± 0.018 μrad yr^{-1} ($\sim 2 \times 10^{-8}$ strain yr^{-1}), an estimate statistically indistinguishable from zero at the 95% confidence level.

More recently regional surveys have been carried out using GPS. Strain accumulation rates have been calculated from changes in angles between monuments first measured by triangulation and then remeasured using GPS. These triangulation/GPS strain rate estimates have been obtained in the NMSZ (Liu et al., 1992; Snay et al., 1994), and MPSSZ (Talwani et al., 1997).

Liu et al. (1992) estimated high shear strain rates

(0.108 ± 0.045 μrad yr^{-1}) for the southern part of NMSZ, including 0.248 ± 0.074 μrad yr^{-1} and 0.111 ± 0.052 μrad yr^{-1} for the western and eastern parts of their study area. In contrast, Snay et al. (1994) obtained 0.030 ± 0.019 μrad yr^{-1} for the northern part of NMSZ, a value indistinguishable from zero at the 95% confidence level. Weber et al. (1998) compared the results of two GPS surveys in 1991 and 1993, encompassing the entire NMSZ. They divided their study area into two subnets. They obtained strain rates of 0.121 ± 0.083 μrad yr^{-1} and 0.080 ± 0.058 μrad yr^{-1} for the two subnets. For the MPSSZ near Charleston, South Carolina, Talwani et al. (1997) obtained 0.041 ± 0.019 μrad yr^{-1}.

In summary, the results of geodetic strain measurements at a regional scale show that within continental interiors there are pockets of high shear strain rate accumulation ~0.02 to 0.2 μrad yr^{-1} (or $\sim 10^{-8}$ to 10^{-7} strain yr^{-1}) compared to the rigid plates ($\sim 10^{-10}$ to 10^{-9} strain yr^{-1}).

1.3. Recurrence rates

The earliest recurrence time estimates for the large earthquakes were based on the extrapolation of the current seismicity data (see e.g., Johnston and Nava, 1985). Now additional estimates of recurrence times are based on deformation rates, and paleoseismicity data. For the NMSZ, Schweig and Ellis (1994) argue for a repeat time of 1000 years or less for the large earthquakes ($\sim M_w$ 8.0). Estimates based on paleoliquefaction data suggest recurrence rates as low as 200–600 yr (Schweig and Tuttle, 1996). For the MPSSZ, estimates of repeat times based on seismicity (and early paleoseismological investigations) range from 1500 to 1800 yr (Talwani and Cox, 1985; Amick and Talwani, 1986; Nishenko and Bollinger, 1990). However, the results of recent paleoseismological investigations (Talwani, 1996) suggest that the repeat time for large earthquakes (M_w 7+) may be about 500 yr.

2. Models for earthquakes in continental interiors

From the preceding paragraphs, I note that the seismicity in continental interiors tends to be clustered, most of it occurring in the upper crust; there are localized pockets of high strain accumulation in an otherwise rigid plate, and the recurrence rate of the large earthquakes is hundreds of years rather than thousands or tens of thousands of years. These observations must be used as constraints in any model presented to explain the seismicity in continental interiors.

Talwani (1989) reviewed various models proposed to explain earthquakes in continental interiors. In common with their plate boundary counterparts, earthquakes within continental interiors, occur when stress overcomes the mechanical strength of that part of the crust. This is accomplished in one or more of the following ways:

(a) Ambient stress grows to exceed the strength of pre-existing zones of weakness.

(b) An additional stress is generated locally, which augments the ambient stress field and triggers earthquakes in continental interiors.

(c) The mechanical strength of the rocks is reduced by mechanical or chemical means.

Examples of the first category include stress amplification near plutons (see e.g., Campbell, 1978), localized strain in the mid–lower crust (Zoback et al., 1985), and stress accumulation near intersecting faults (Talwani, 1988). The second category includes models for local generation of triggering stress. These include changes in the stress field due to deglaciation (see e.g., Quinlan, 1984) and gravitationally induced stresses at structural boundaries (Goodacre and Hasegawa, 1980). In the third category, there is a reduction in strength of rocks by mechanical or chemical means. Models include those proposed to explain induced seismicity (see e.g., Talwani, 1997), e.g., by an increase in fluid pressures, stress corrosion, dissolution and by a lowering of the coefficient of friction.

Recent models to explain seismicity in the Amazonas region in Brazil (Zoback and Richardson, 1996) and in the NMSZ (Stuart et al., 1997) are variations of the second category, in that a mechanism is proposed to build-up stress locally. However in both cases, the source of the stress build-up is in the lower crust.

2.1. The fault intersection model

In the intersection model (Talwani et al., 1979; Illies, 1982; Talwani, 1988) the intersection of two

or more zones of weakness provides a location for stress build-up. The intersecting zone may be local in nature, e.g. the boundary fault of a buried basin, or it may be regional in scale (see e.g., Marshak and Paulsen, 1997), such as a major tectonic boundary or an ancient rift zone. The boundaries of crustal blocks, which often separate rocks with different rheological properties, form fault intersections, the local weak spots. These are characterized by an increased density of fractures of various orientations as evidenced by focal mechanisms, higher seismicity and lower magnitudes. Fault intersections are also associated with increased permeability, promoting fluid flow and higher fluid pressure generation (see e.g., Sibson, 1988).

The intersections form the locked area of a fault and are the locations of stress build-up. Because movement on one fault is inhibited by the intersecting fault, stresses large enough to generate a major intraplate earthquake can build up at intersections. Intersections also help to localize the seismicity and as noted by King (1986), form the location where seismicity is initiated. The faulting usually starts on one of the fault planes and due to the movement on it perturbs the neighboring stress field and triggers movement on the adjacent fault.

Laboratory and field data (Ma et al., 1989; Ellis, 1991) show that stress accumulation occurs in asymmetric lobes around the intersection. Numerical analysis by Andrews (1989) showed that after a number of earthquakes, the junction becomes a strong barrier to further slip and the largest slip occurs away from the intersection on one or both of the intersecting faults. Further analysis by Andrews (1994) also predicts a volume change or intense local deformation at the intersection. These predictions are consistent with the observation of seismicity in continental interiors, where the mainshock occurs away from the intersection (Talwani, 1988), while intense seismicity often accompanied by uplift occurs near the intersection.

Jing and Stephansson (1990) modeled the stress build-up near intersecting faults using a two-dimensional distinct element method. Their model consisted of three blocks, one of which (block 3) was kept fixed (Fig. 1a). In response to a compressional stress field (similar to that observed in eastern North America), a non-uniform stress distribution is gen-

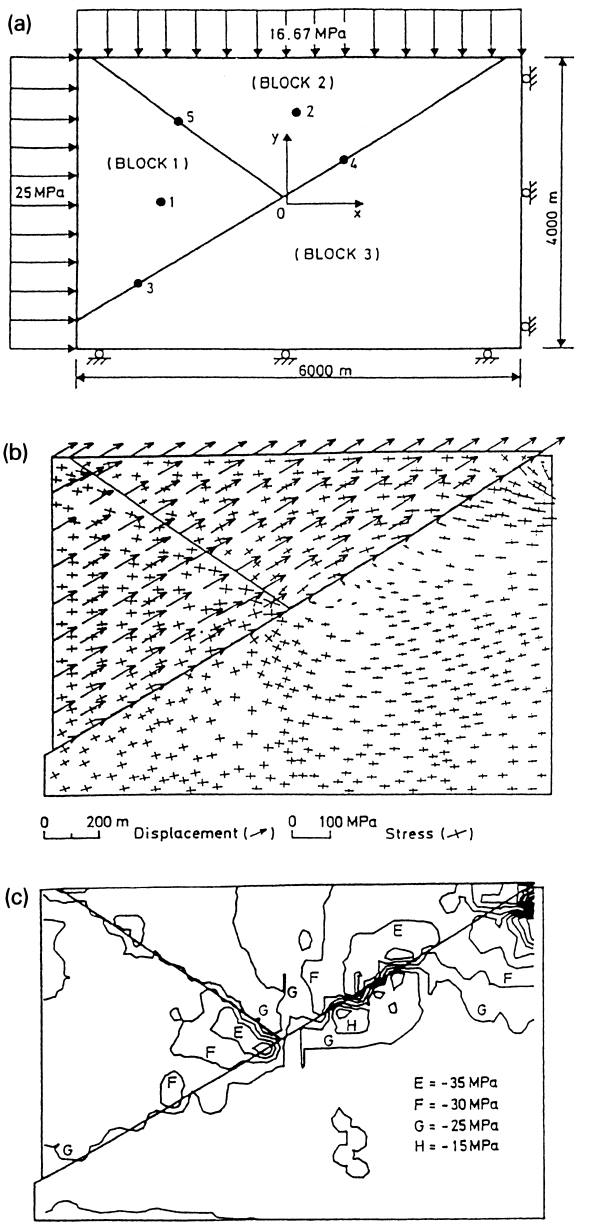

Fig. 1. Results of numerical modeling by 2-D distinct element model (from Jing and Stephansson, 1990). (a) Block geometry and boundary conditions, and location of monitoring points for the computational model. Blocks 1 and 2 are allowed to move and block 3 is kept fixed. (b) Principal stress components and displacement vectors. Note that blocks 1 and 2 move in a right-lateral sense and that principal stress components suggest a rotational stress field in block 3. (c) Contours of normal stress, S_x. Negative stresses are compressional. Model yields a stress field favoring right-lateral slip between blocks 2 and 3 and left-lateral slip between blocks 1 and 2.

erated, and the two movable blocks (1 and 2) move in a right-lateral sense (Fig. 1b). Fig. 1c shows the contours of the horizontal normal stress S_x. I note that stress concentrations occur near the intersection. Jing and Stephansson (1990) follow the engineering stress sign convention, negative values indicating compression. The stress field would support right-lateral slip on the upper two blocks relative to block 3, which is fixed and left lateral movement of block 1 relative to block 2.

In Fig. 2, I have replotted the results of Jing and Stephansson (1990) rotating the blocks by 180°. Fig. 2a–d show the block model (block 3 fixed), contours of S_x, displacement vectors and principal stress components, respectively. In block 3, I note that the stress field would favor rotation. In Fig. 2e, I allow block 3 to move. As a result of the stress accumulation a split occurs at B and block 1 moves in a left-lateral sense with respect to block 2. The left-lateral displacement of block 1, BB′, is limited, as for the given stress field it is easier for block 3 to move in a right-lateral sense. On further application of the stress field, legs AB and B′C move in a right-lateral sense, uplift occurs along BB′ and leg B′C undergoes anticlockwise rotation (Fig. 2f). The uplift along BB′ is also consistent with analyses of Andrews (1994). (In an extensional stress field, S_x directed outward, one would anticipate normal faulting and subsidence along BB′). Thus Fig. 2f shows the resultant geometry (with leg B′C undergoing rotation) of the intersecting blocks (Fig. 2a) subjected to a compressional stress field commonly observed in continental interiors.

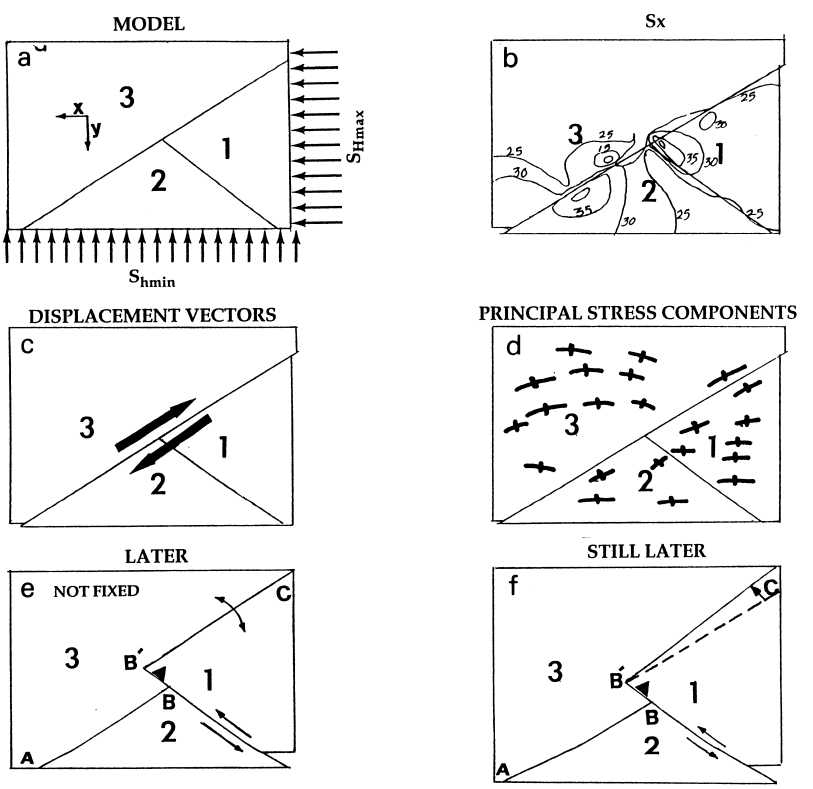

Fig. 2. The model of Jing and Stephansson (1990) modified and rotated by 180°. S_{Hmax} and S_{hmin} are the maximum and minimum stresses. (a–d) The model, contours of S_x, displacement vectors and principal stress components. (e) Block 3 is allowed to move and leads to an offset of *BB′* in fault *AC* and beginning of uplift (solid triangle) along the offset and rotation of leg *B′C*. (f) The final geometry of the intersecting faults.

2.2. Three examples

In Fig. 3, I show schematically, the geometry of three well studied locations of seismicity in continental interiors, each with a geometry similar to that in Fig. 2f. Intriguingly at each of these locations there was a sequence of three earthquakes or subevents. Each of these three events occurred on a different fault.

Fig. 3a shows the geometry of the fault system in the New Madrid Seismic Zone, modified from Gomberg (1992) and using nomenclature from Johnston and Schweig (1996). The two NE–SW segments, BA (Blytheville Arch) and NN (New Madrid North) are associated with right-lateral strike-slip faulting and the intersecting northwest trending NW (New Madrid Northwest) is associated with reverse faulting and the Lake County Uplift. The BA leg is oriented at about 27° to the direction of maximum horizontal compression, S_{Hmax} (N80°E), whereas the NN leg is rotated 10° anticlockwise, with respect to BA, and makes an angle of about 37° with S_{Hmax}. According to Johnston and Schweig (1996) the 1811–1812 sequence started on the BA leg (12/1811), and was followed by large events on the NN and NW legs (1/1812 and 2/1812).

Fig. 3b shows the geometry of the fault system in the Middleton Place Summerville Seismic Zone, with nomenclature from Talwani (1982) and locations from Garner (1998). Here also the N10°–15°E trending Woodstock fault is offset ~3–4 km to the NW by the northwest trending Ashley River fault. S_{Hmax} is oriented N60°E. The region south of Summerville (SV in Fig. 3b) is uplifted (Rhea, 1989; Marple and Talwani, 1993) and is currently associated with reverse faulting. The northern leg of the Woodstock fault is rotated ~5° anticlockwise with respect to the southern leg.

The 1886 earthquake was studied in great detail by Sloan who was employed by the U.S. Geological Survey. His reports to McGee were later made available to Dutton (1890), who published the main report on the 1886 Charleston earthquake. In Dutton's interpretation the earthquake was bipolar (consistent with the then prevailing theory of earthquakes) and had two 'epicentra' located near Woodstock and Rantowles. (These towns are located 12 and 22 km to the southeast and south of Summerville). However, in his original report (see e.g., McKinley (1887), in the Charleston yearbook for 1886), Sloan argues for a 'compound shock' and lists three 'foci' near Woodstock, Middleton Place and Rantowles. The second source, Middleton Place lies on the Ashley River fault and is currently associated with reverse faulting. Thus the original data collected after the 1886 point to three earthquakes on different faults.

Fig. 3c shows the geometry of the faults associated with the M_S 7.3 Haicheng earthquake of 1975 (Jones et al., 1982). The foreshocks (F) occurred near the intersection of the Dayanghe (striking N45°W) and Ximuhe faults. The magnitude of the largest foreshock was M_S 4.7 (Wu et al., 1978). The mainshock (M) occurred near the intersection of the Ximuhe and a northwest trending fault (striking

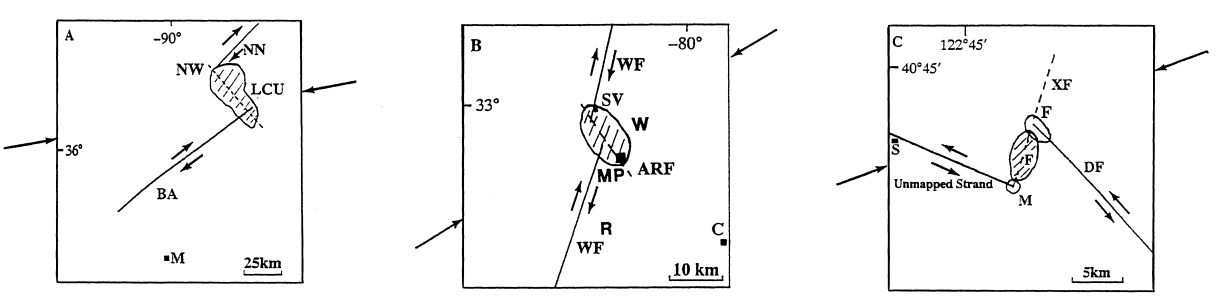

Fig. 3. Schematic geometry of three locations of continental interior earthquakes. The solid arrows show the direction of S_{Hmax}. (a) NMSZ, where *BA*, *NW*, *NN*, *LCU* and *M* are Blytheville Arch, northwest and north New Madrid faults, Lake County Uplift and Memphis, respectively. (b) MPSSZ, where *WF* and *ARF* are the Woodstock and Ashley River faults, respectively. *W*, *MP*, *R*, *SV* and *C* are Woodstock, Middleton Place, Rantowles, Summerville and Charleston, respectively. (c) Haicheng, China, *DF*, *XF* are the Dayanghe and Ximuhe faults, respectively. *F*, *M* and *S* are locations of foreshocks, mainshocks and Shipengyu, respectively. Aftershocks were used to define the 'unmapped' strand.

N67ºW), the latter being associated with the aftershock activity. This fault was labeled 'unmapped' fault by Jones et al. (1982). The magnitude of the largest aftershock was M_s 6.0 (Ma et al., 1989). Triangulation surveys before and after the mainshock revealed shortening (and hence uplift) in an area between the two northwest trending faults (Wu et al., 1978). The direction of S_{Hmax}, N70ºE is from Wu et al. (1978), and I note that the western leg of the two northwest trending faults is rotated about 22º anticlockwise with respect to the eastern leg.

3. Discussion

Johnston and Schweig (1996) noted that earthquake triplets, with each principal shock generating its own aftershock series, are relatively common in intraplate settings, in contrast with large interplate earthquakes which are usually associated with mainshock–aftershock sequences. In addition to the 1811–1812 sequence of earthquakes in the NMSZ, Johnston and Schweig (1996) cite examples of earthquake triplets for the 1990 Sudan; 1976–84 Gazli, Uzbekistan; 1985–88 Nahani, Canada; 1988 Tennant Creek, Australia; and the 1982 Miramichi, New Brunswick sequences. The actual style of faulting at any location depends (among other factors) on the strike and dip of a fault plane and its orientation with respect to S_{Hmax}. Hence, although the style of faulting on individual faults varies from one location to another, at locations where adequate data are available, faulting was localized near intersecting faults which displayed nonuniform styles of faulting, and evidence of uplift near the intersections.

In the three examples presented here I find a similar geometrical relationship of the intersecting faults with each other and with the direction of S_{Hmax}. The shorter intersecting fault appears to divide the longer fault into two segments offset from each other along the intersecting fault. I observed strike-slip faulting on the longer fault segments favorably oriented to S_{Hmax} and reverse faulting and/or uplift on the shorter (intersecting) fault. At the intersection, the offsetting fault appears to be most heavily fractured and is associated with intense seismicity, whereas the larger event(s) occur on the two offset faults (see e.g., Johnston, 1982; Garner, 1998; and Wu et al., 1978).

Next, using the seismicity near Charleston as an example, I show that the observed strain rate and recurrence time are adequate to generate the 1886 M_w 7.3 earthquake. The strain rate observed from GPS $\sim$0.04 μrad yr^{-1} was measured over a GPS array with an aperture of $\sim$100 km, leading to a slip-rate of $\sim$4 mm/yr. For an average recurrence time of $\sim$500 years, the anticipated slip in one earthquake cycle is $\sim$2 m, a number consistent with the observed shortening of railroad tracks in the 1886 Charleston earthquake (Charleston News and Courier, September 5, 1886, p. 1 col. 6), and also roughly consistent with the average slip expected for M_w $\sim$7.0–7.5 earthquakes with average stress drop (Johnston, 1993).

4. Conclusions

In this speculative model, intersecting faults in the upper crust provide a location for stress accumulation in continental interiors. GPS surveys can be used to detect these localized pockets of high strain in an otherwise low-strain plate interior.

In three examples presented in this paper, the shorter intersecting fault divided and offset the longer fault. In all examples one of the two segments of the longer fault underwent rotation with respect to the other. The sense of rotation is consistent with analytic models by Andrews (1989, 1994) and Jing and Stephansson (1990). The type of displacement on the outer faults was strike-slip faulting in all three examples. In each case faults were oriented $\sim$45º $\pm$ 15º from S_{Hmax}. For cases where the fault orientation is steeper, close to perpendicular to S_{Hmax}, I would anticipate reverse faulting on the 'main' faults, e.g., the earthquakes near Tennant Creek, Australia and Latur, India.

In this paper I have focussed on the stress build-up near intersecting faults in continental interiors. Another consequence of the geometry of the faults, and one which plays an important role in localizing earthquakes is stress transfer and loading and unloading of neighboring faults due to an earthquake on one fault (see e.g., King et al., 1994). It is thus possible, in fact likely, that transient stress triggering played an integral role in the occurrence of the series of earthquakes on adjacent faults described in the three examples.

The ideas presented in this model are not scale-dependent and would also apply to intermediate-size earthquakes. The validity of the model will be tested with additional data from other locations of earthquakes in continental interiors.

Acknowledgements

I thank Steve Marshak and Michael Hamburger for helpful comments on the manuscript and for inviting me to attend the Penrose Conference. I also want to thank Arch Johnston for sharing his insight with me and for his comments.

References

Amick, D., Talwani, P., 1986. Earthquake recurrence rates and probability estimates for the occurrence of significant seismic activity in the Charleston area: The next 100 years. Proc. 3rd U.S. Natl. Conf. Earthquake Engineering. EERI, Charleston, SC, Vol. I, 55–64.

Anderson, J.G., 1986. Seismic strain rates in the central and eastern United States. Bull. Seismol. Soc. Am. 76, 273–290.

Andrews, D.J., 1989. Mechanics of fault junctions. J. Geophys. Res. 94, 9389–9397.

Andrews, D.J., 1994. Fault geometry and earthquake mechanics. Ann. Geofis. 37, 1341–1348.

Campbell, D.L., 1978. Investigation of the stress-concentration mechanism for intraplate earthquakes. Geophys. Res. Lett. 5, 477–479.

Dixon, T.H., Mao, A., Stein, S., 1996. How rigid is the stable interior of the North American plate? Geophys. Res. Lett. 23, 3035–3038.

Dutton, C.E., 1890. The Charleston earthquake of August 31, 1886. U.S. Geol. Surv., 9th Annu. Rep. 1887–1888, pp. 203–528.

Ellis, W.L., 1991. Stress distribution in South Central Oklahoma and its relationship to crustal structure and contemporary seismicity. In: Roegiers, J.-C. (Ed.), Proc. 32nd U.S. Symp. Rock Mechanics. Balkema, Rotterdam, pp. 73–81.

Garner, J.T., 1998. Re-evaluation of the seismotectonics of the Charleston, South Carolina area. Ms. thesis, Univ. South Carolina, Columbia, SC, 250 pp.

Girdler, R.W., McConnell, D.A., 1994. The 1990 to 1991 Sudan earthquake sequence and the extent of the East African Rift System. Science 264, 67–70.

Gomberg, J., 1992. Tectonic deformation in the New Madrid seismic zone: Inferences from boundary element modeling. Seismol. Res. Lett. 63, 407–426.

Goodacre, A.K., Hasegawa, H.S., 1980. Gravitationally induced stresses at structural boundaries. Can. J. Earth Sci. 17, 1286–1291.

Hudnut, K.W., Seeber, L., Pacheo, J., 1989. Cross-fault triggering in the November 1987 Superstition Hills earthquake sequence, Southern California. Geophys. Res. Lett. 16, 199–202.

Illies, J.H., 1982. Der Hohenzollern Graben und Intraplatten-Seismizität infolge Vergitterung lamellärer Scherung mit einer Riftstruktur. Oberrhein. Geol. Abh. 31, 47–78.

Jing, L., Stephansson, O., 1990. Numerical modelling of intraplate earthquake by 2-dimensional distinct element method. Gerlands Beitr. Geophys. 99, 463–472.

Johnston, A.C., 1982. A major earthquake zone on the Mississippi. Sci. Am. 246, 60–68.

Johnston, A.C., 1993. Average stable continental earthquake source parameters based on constant stress drop scaling. Seismol. Res. Lett. 64, 261 (Abstract).

Johnston, A.C., 1994. Seismotectonic interpretations and conclusions from the stable continental region seismicity data base. In: The Earthquakes of Stable Continental Regions. Vol. 1: Assessment of Large Earthquake Potential. Electr. Power Res. Inst., Palo Alto, CA, 4-1-4-103.

Johnston, A.C., Nava, S.J., 1985. Recurrence rates and probability estimates for the New Madrid seismic zone. J. Geophys. Res. 90, 6737–6753.

Johnston, A.C., Schweig, E.S., 1996. The enigma of the New Madrid earthquakes of 1811–1812. Annu. Rev. Earth Planet. Sci. 24, 339–384.

Jones, L.M., Wang, B., Xu, S., Fitch, T.J., 1982. The foreshock sequence of the February 4, 1975, Haicheng earthquake ($M = 7.3$). J. Geophys. Res. 87, 4575–4584.

King, G.C.P., 1986. Speculations on the geometry of the initiation and termination processes of earthquake rupture and its relation to morphological and geological structure. Pageoph 124, 567–585.

King, G.C.P., Stein, R.S., Lin, J., 1994. Static stress changes and the triggering of earthquakes. Bull. Seismol. Soc. Am. 84, 935–953.

Liu, L., Zoback, M.D., Segall, P., 1992. Rapid intraplate strain accumulation in the New Madrid seismic zone. Science 257, 1666–1669.

Ma, Z., Fu, Z., Zhang, Y., Wang, C., Zhang, G., Liu, D., 1989. Earthquake Prediction. Nine Major Earthquakes in China (1966–1976). Seismological Press, Beijing. (English translation)

Marple, R.T., Talwani, P., 1993. Evidence of possible tectonic upwarping along the South Carolina Coastal Plain from an examination of river morphology and elevation data. Geology 21, 651–654.

Marshak, S., Paulsen, T., 1997. Structural style, regional distribution, and seismic implications of Midcontinent fault-and-fold zones, United States. Seismol. Res. Lett. 68, 511–520.

McKinley, C., 1887. A descriptive narrative of the earthquake of August 31, 1886. Appendix for the City (of Charleston) Yearbook, 1886, pp. 345–441.

Nishenko, S.P., Bollinger, G.A., 1990. Forecasting damaging earthquakes in the central and eastern United States. Science 249, 1412–1416.

Quinlan, G., 1984. Postglacial rebound and the focal mechanisms

of eastern Canadian earthquakes. Can. J. Earth Sci. 21, 1018–1023.

Rhea, S., 1989. Evidence of uplift near Charleston, South Carolina. Geology 17, 311–315.

Robbins, J.W., Smith, D.E., Ma, C., 1993. Horizontal crustal deformation and large scale plate motions inferred from space geodetic techniques. In: Smith, D.E., Turcotte, D.L. (Eds.), Contributions of Space Geodesy to Geodynamics: Crustal Dynamics. Geodynamics Ser. 23, Am. Geophys. Union, pp. 21–36.

Savage, J.C., 1983. Strain accumulation in western United States. Annu. Rev. Earth Planet. Sci. 11, 11–42.

Schweig, E.S., Ellis, M.A., 1994. Reconciling short recurrence intervals with minor deformation in the New Madrid seismic zone. Science 264, 1308–1311.

Schweig, E.S., Tuttle, M.P., 1996. Paleoseismology and earthquake recurrence in the New Madrid seismic zone: Are the apparent rates reasonable? Seismol. Res. Lett. 67, 54 (Abstract).

Sibson, R.H., 1988. Earthquake faulting, induced fluid flow, and fault-hosted gold-quartz mineralization. In: Bartholomew, M.J., Hyndman, D.W., Mogk, D.W., Mason, R. (Eds.), Basement Tectonics: Characterization and Comparison of Ancient and Mesozoic Continental Margins. Proc. 8th Int. Conf. Basement Tectonics, Butte, MT, pp. 603–614.

Snay, R.A., 1986. Horizontal deformation in New York and Connecticut: Examining contradictory results from the geodetic evidence. J. Geophys. Res. 91, 12695–12702.

Snay, R.A., Strange, W.E., 1997. Horizontal velocities in the central and eastern United States from GPS surveys during the 1987–1996 interval. NUREG/CR-6586, U.S. Nucl. Regul. Comm. Washington, D.C. 20555, 27 pp.

Snay, R.A., Ni, J.F., Neugebauer, H.C., 1994. Geodetically derived strain across the northern New Madrid seismic zone. In: Shedlock, K.M., Johnston, A.C. (Eds.), Investigations of the New Madrid Seismic Zone. U.S. Geol. Surv. Prof. Pap. 1538-F, pp. F1–F6.

Stein, S., 1993. Space geodesy and plate motions. In: Smith, D.E., Turcotte, D.L. (Eds.), Space Geodesy and Geodynamics. Geodynamics Ser. 23, Am. Geophys. Union, pp. 5–20.

Stuart, W.D., Hildenbrand, T.G., Simpson, R.W., 1997. Stressing of the New Madrid seismic zone by a lower crust detachment fault. J. Geophys. Res. 102, 27623–27633.

Talwani, P., 1982. An internally consistent pattern of seismicity near Charleston, South Carolina. Geology 10, 654–658.

Talwani, P., 1988. The intersection model for intraplate earthquakes. Seismol. Res. Lett. 59, 305–310.

Talwani, P., 1989. Characteristic features of intraplate earthquakes and the models proposed to explain them. In: Gregersen, S., Basham, P.W. (Eds.), Earthquakes at North-Atlantic Passive Margins: Neotectonics and Post-Glacial Rebound. NATO ASI Ser. C, Mathematical and Physical Sciences, pp. 563–579.

Talwani, P., 1996. Prehistoric earthquakes in the South Carolina Coastal Plain. Geol. Soc. Am. Abstr. Programs 28, A283.

Talwani, P., 1997. On the nature of reservoir-induced seismicity. Pageoph 150, 473–492.

Talwani, P., Cox, J., 1985. Paleoseismic evidence for recurrence of earthquakes near Charleston, South Carolina. Science 229, 379–381.

Talwani, P., Amick, D.C., Logan, R., 1979. A model to explain the intraplate seismicity in the South Carolina Coastal Plain. Eos Trans. Am. Geophys. Union 60, 311 (Abstract).

Talwani, P., Kellogg, J.N., Trenkamp, R., 1997. Validation of tectonic models for an intraplate seismic zone, Charleston, South Carolina, with GPS geodetic data. NUREG/CR-6529, U.S. Nucl. Regul. Comm., Washington, D.C. 20555, 41 pp.

Weber, J., Stein, S., Engeln, J., 1998. Estimation of intraplate strain accumulation in the New Madrid seismic zone from repeat GPS surveys. Tectonics 17, 250–266.

Wu, K., Yue, M., Wu, H., Can, X., Chen, H., Huang, W., Tian, K., Lu, S., 1978. Certain characteristics of Haicheng earthquake ($M = 7.3$) sequence. Chin. Geophys. 1, 289–308 (English translation).

Zoback, M.D., Prescott, W.H., Krueger, S.W., 1985. Evidence for lower crustal ductile strain localization in southern New York. Nature 317, 705–707.

Zoback, M.L., Richardson, R.M., 1996. Stress perturbation associated with the Amazonas and other ancient continental rifts. J. Geophys. Res. 101, 5459–5475.